



THE UNIVERSITY *of* EDINBURGH

Edinburgh Research Explorer

## Attribution of detected temperature trends in Southeast Brazil

**Citation for published version:**

de Abreu, C, Tett, S, Schurer, A & Rocha, HR 2019, 'Attribution of detected temperature trends in Southeast Brazil', *Geophysical Research Letters*. <https://doi.org/10.1029/2019GL083003>

**Digital Object Identifier (DOI):**

[10.1029/2019GL083003](https://doi.org/10.1029/2019GL083003)

**Link:**

[Link to publication record in Edinburgh Research Explorer](#)

**Document Version:**

Publisher's PDF, also known as Version of record

**Published In:**

Geophysical Research Letters

**General rights**

Copyright for the publications made accessible via the Edinburgh Research Explorer is retained by the author(s) and / or other copyright owners and it is a condition of accessing these publications that users recognise and abide by the legal requirements associated with these rights.

**Take down policy**

The University of Edinburgh has made every reasonable effort to ensure that Edinburgh Research Explorer content complies with UK legislation. If you believe that the public display of this file breaches copyright please contact [openaccess@ed.ac.uk](mailto:openaccess@ed.ac.uk) providing details, and we will remove access to the work immediately and investigate your claim.



# Geophysical Research Letters

## RESEARCH LETTER

10.1029/2019GL083003

### Key Points:

- New detection and attribution method is used to attribute temperature trends for Southeast Brazil
- Greenhouse gases are the dominant driver of observed temperature trends
- Model uncertainty plays an important role in this study

### Supporting Information:

- Supporting Information S1

### Correspondence to:

R. C. de Abreu,  
rafael.abreu@iag.usp.br



### Citation:

de Abreu, R. C., Tett, S. F. B., Schurer, A., & Rocha, H. R. (2019). Attribution of detected temperature trends in Southeast Brazil. *Geophysical Research Letters*, 46. <https://doi.org/10.1029/2019GL083003>

Received 25 MAR 2019

Accepted 10 JUL 2019

## Attribution of Detected Temperature Trends in Southeast Brazil

R. C. de Abreu<sup>1</sup> , S. F. B. Tett<sup>2</sup>, A. Schurer<sup>2</sup> , and H. R. Rocha<sup>1</sup>

<sup>1</sup>Instituto de Astronomia, Geofísica e Ciências Atmosféricas, Universidade de São Paulo, São Paulo, Brazil, <sup>2</sup>School of Geosciences, University of Edinburgh, Edinburgh, UK

**Abstract** Southeast Brazil has great economic importance for Brazil and is highly vulnerable to extreme events like floods and droughts. Studies have shown an increase of temperature in this region. Using a new detection and attribution framework (Ribes et al., 2017, <https://doi.org/10.1007/s00382-016-3079-6>) and Coupled Model Intercomparison Project Phase 5 models, this change is found to be largely due to greenhouse gases. We estimate that greenhouse gases contribute a warming of 0.95 to 1.5 °C to the observed warming trend of 1.1 °C between 1955 and 2004. Temperature changes from natural and nongreenhouse gas anthropogenic forcing are estimated to be small over this period. Results are robust using different time windows. Using the Community Earth System Model ensembles to evaluate the impacts of internal variability, observational and model error shows that most uncertainty arises from model error.

**Plain Language Summary** Southeast Brazil has great economic importance for Brazil and is highly vulnerable to extreme events like floods, droughts, and heat waves. Many studies link those kind of events with an increase in temperature due to climate change, largely caused by increasing atmospheric concentrations of greenhouse gases. This study tested whether or not human-induced climate change is responsible for the observed increase in temperature in Southeast Brazil. The observed 1.1 °C per 50-year trend is largely due to increasing greenhouse gases, which means that they have a significant role in observed changes in Southeast Brazilian temperatures.

## 1. Introduction

Southeast Brazil is the geopolitical region in Brazil that comprises the states of São Paulo, Rio de Janeiro, Minas Gerais, and Espírito Santo and is responsible for more than 50% of Brazil Gross Domestic Product with a broad range of economic activities that includes agriculture, mineral extraction, automobile industries, and others (IBGE, 2018b). More than 40% of Brazil's population lives in this region, and it contains two of the most important cities of the country, São Paulo and Rio de Janeiro (IBGE, 2018a). The high exposure makes the region vulnerable to changes in climate, like droughts in major cities (Coelho et al., 2016) and impacts on agricultural production due to an increase of temperature (Camargo, 2010; Marengo, 2001).

The fifth assessment report of the Intergovernmental Panel on Climate Change reported an observed global warming of 0.85 [0.65 to 1.06] °C between 1880 and 2012. In Brazil, studies have shown an increase of more than 3 °C in the city of São Paulo between 1940 and 2010 (Silva Dias et al., 2013). Also, the frequency of warm nights (minimum temperature above 90% percentile) has increased while cold nights (minimum temperature below 10% percentile) have decreased with statistically significant trends over Southeast Brazil (Vincent et al., 2005). Other observational studies have been made in South America and on individual cities in the state of São Paulo, to analyze whether a change in temperature could be detected and if these were due to increasing greenhouse gases (GHG) and other forcings (Blain et al., 2009; Marengo, 2001). Although these studies find statistically significant trends in observations, the authors suggest that these changes could be either due to increase in GHG from climate change or local factors like urbanization and land use changes from agricultural production that could have a significant impact on observed trends.

The question of whether anthropogenic climate change has driven temperature trends has been investigated in many studies, where the causal relation between climate forcings and observed changes is evaluated (Bindoff et al., 2013). The common approach is to use linear regression models called optimal fingerprint

(Allen & Stott, 2003; Allen & Tett, 1999; Hegerl et al., 1996) where scaling factors on simulated signals are estimated with a range of uncertainty. The magnitude of the scaling factor and its confidence interval is then used to make inferences about the causation of the external forcing in the observed changes. Although some Detection and Attribution (D&A) studies have been made for particular weather events in Brazil (de Abreu et al., 2019; Otto et al., 2015), no long-term change attribution studies have been conducted in South America. Further, few D&A studies have been made to attribute human-induced climate change in subnational scale as done here. We could only find three recent studies (Wang et al., 2017; Wan et al., 2019; Wang et al., 2018). These studies found a human influence in temperature trends in Western China, regional Canadian change, and in extreme temperature indices in 17 subcontinent regions around the world. The study of Karoly and Stott (2006) also detected a human influence on Central England temperature. Therefore, this study aims to answer the question of whether observed temperature changes in Southeast Brazil can be attributed to human and natural forcings.

## 2. Methods

### 2.1. Attribution Model

The statistical model used for attribution of climate change in Southeast Brazil is that of Ribes et al. (2017), here after called R17. R17 assumes that the true observed climate response ( $Y^*$ ) is a sum of true responses from each individual forcing ( $X_i^*$ )

$$Y^* = \sum_{i=1}^{n_f} X_i^*, \quad (1)$$

$$Y = Y^* + \epsilon_Y, \quad (2)$$

$$X_i = X_i^* + \epsilon_{X_i}, \quad (3)$$

where  $Y$  is the observation vector,  $X_i$  is the simulated individual forcing vector,  $\epsilon_Y \sim N(0, \Sigma_Y)$  is observational uncertainty, and  $\epsilon_{X_i} \sim N(0, \Sigma_{X_i})$  is model uncertainty, with their respective covariance matrices  $\Sigma_Y$  and  $\Sigma_{X_i}$ . We assume that observational uncertainty arises from internal variability and observational error, while  $\epsilon_{X_i}$  arises from internal variability and model uncertainty. Since both errors are assumed to be Gaussian,  $X_i^*$  and  $Y^*$  can be estimated using Maximum Likelihood Estimators with exact confidence intervals as

$$\hat{Y}^* = Y + \Sigma_Y(\Sigma_Y + \Sigma_X)^{-1}(X - Y) \sim N(Y^*, (\Sigma_X^{-1} + \Sigma_Y^{-1})^{-1}), \quad (4)$$

$$\hat{X}_i^* = X_i + \Sigma_{X_i}(\Sigma_Y + \Sigma_X)^{-1}(Y - X) \sim N(X_i^*, (\Sigma_{X_i}^{-1} + (\Sigma_Y + \sum_{j \neq i} \Sigma_{X_j})^{-1})^{-1}), \quad (5)$$

where  $\Sigma_X = \sum_{i=1}^{n_f} \Sigma_{X_i}$  and  $X = \sum_{i=1}^{n_f} X_i$ . To check for consistency between the observed signal with any set of forcings,  $\chi^2$  tests are used as discussed in R17. First, this test is used to detect consistency with internal variability only (equation (6)) and all of those response patterns are tested to detect consistency between observations and the analyzed forcings (equation (7)). Consistency of observations with the response to individual forcing is also tested using equation (7).

$$Y' \Sigma_Y^{-1} Y \sim \chi^2(n), \quad (6)$$

$$(Y - X)'(\Sigma_Y + \Sigma_X)^{-1}(Y - X) \sim \chi^2(n), \quad (7)$$

where  $n$  is the size of  $Y$ . As in R17 study, ordinary least square (OLS; Allen & Tett, 1999) is also used to compare the results found with the R17 methodology. The OLS method assumes a linear relation between the simulated responses  $X_i$  and the observed one  $Y$ . A scaling factor  $\beta$  is then estimated by  $\hat{\beta}_{OLS}$  which can be used for inference

$$Y = X\beta + \epsilon_Y, \quad (8)$$

$$\hat{\beta}_{OLS} = (X^T \Sigma_Y^{-1} X)^{-1} X^T \Sigma_Y^{-1} Y. \quad (9)$$

The main differences between the R17 method and OLS is that R17 does not include a scaling factor but does explicitly include observational and model uncertainty. Therefore,  $\epsilon_Y$  in OLS is calculated using only internal variability.

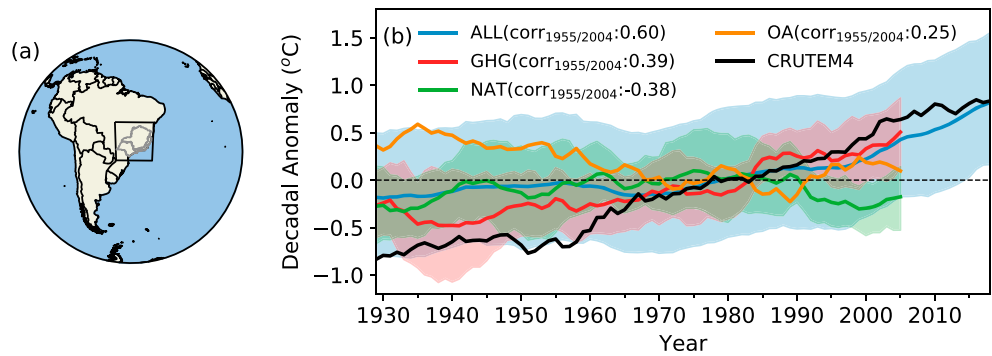


**Figure 1.** (a) Region of interest comprising all states in Southeast Brazil highlighted by the black box bounded by 53.4°W, 26.5°S and 39°W, 12.7°S. (b) The 10-year moving average of annual temperature anomalies, between 1920 and 2017 for CRUTEM4 (black line), ALL (blue line), GHG (red line), and NAT (green line) simulations. Other Anthropogenic (OA; orange line) is ALL minus GHG and NAT ensemble means. Shading indicates the model spread (5% to 95% range). Correlations between CRUTEM4 annual anomalies and 1955–2004 ensemble means are displayed in the labels. The anomalies are calculated with respect to 1961 to 1990 climatology.

## 2.2. Covariance Matrices

Estimation of  $Y^*$  and  $X_i^*$  in equations (4) and (5), respectively, requires inverting covariance matrices:  $\Sigma_Y$  and  $\Sigma_{X_i}$ . A first guess would be to use the sample covariance matrix  $\hat{\Sigma} = \hat{\Sigma}_E = ZZ^T/n$ , where  $Z$  is a  $p \times n$  matrix of  $p$  successions of vectors of pseudo-observations with  $n$  observations. However, in the case when  $p > n$ ,  $\hat{\Sigma}$  is noninvertible. Approaches used in the literature, instead of using  $\hat{\Sigma}_E$ , are the Moore-Penrose pseudo-inverse (Allen & Tett, 1999; Hegerl et al., 1996) or regularization of the covariance matrix (Ribes et al., 2009, 2013). The first approach involves truncating  $\hat{\Sigma}$  to the first  $k$  leading empirical orthogonal functions, while the second involves a linear combination given by

$$\hat{\Sigma} = \rho I_p + \lambda \hat{\Sigma}_E, \quad (10)$$

where  $I_p$  is the  $p \times p$  identity matrix and  $\rho$  and  $\lambda$  are real numbers. This regularization approach is used in this study to provide a better estimate of the sample covariance matrix, and the estimation of  $\rho$  and  $\lambda$  are as Ledoit and Wolf (2004) used in Ribes et al. (2009, 2013). In regularization the choice of  $\rho$  and  $\lambda$  is important because depending on their values, it might lower the variance and increase the bias. However, Ledoit and Wolf (2004) method showed indications of leading to a more powerful statistical test, with a lower mean squared error, and is more objective than truncating to the leading  $k$  eigenvectors, which depends on the choice of  $k$  (Ribes et al., 2009).

## 3. Data and Preprocessing

Gridded temperature observations from the Climatic Research Unit Temperature, version 4 data set (CRUTEM4) are used in this study to estimate the observed trends in temperature for Southeast Brazil. This data set uses homogenized weather stations, has been corrected for urbanization effects, and provides monthly anomalies on a  $5^\circ \times 5^\circ$  latitude/longitude grid from 1850 to present (Jones et al., 2012). The area selected for this study comprises all of the land in Southeast Brazil, bounded by 53.4°W, 26.5°S and 39°W, 12.7°S (Figure 1a).

Annual averages of the area-averaged monthly anomalies were computed following the procedure described in Morice et al. (2012). We focus on three distinct periods: 1955 to 2004, 1935 to 2004, and 1955 to 2014. The first period was selected because it is when the trend is more significant, observations are more reliable (Figure S1 in the supporting information), and simulated signals for different forcings are available. The second period was selected as a sensitivity test with a longer period of data. The third period expands the analysis for 10 years to include a clear signal of the detected trend using only the all forcings simulation. For 2005 to 2014 simulations using Representative Concentration Pathway 8.5 from the models of the Coupled Model Intercomparison Project Phase 5 (CMIP5; Table S1) were used. The 10-year averages were then computed and the temporal mean subtracted from the data in order to focus only on the anomalies following Ribes et al. (2013). Therefore, the sizes of the vectors  $X_i$  and  $Y$  are five for the 1955–2004 period, seven for 1935–2004, and six for 1955–2014.

In this study we use simulations from the Community Earth System Model (Hurrell et al., 2013) to understand which of the various uncertainties (internal variability, observational error, and model error) are more important. We use 34 members from the large ensemble (CESM-LE; Kay et al., 2015) driven with both natural and anthropogenic forcings (ALL), a three-member ensemble with solar and volcanic forcings (NAT), and a three-member ensemble driven only with GHG. Simulated data are interpolated to the CRUTEM4  $5^\circ \times 5^\circ$  grid and masked by the observational monthly mean data set. The CMIP5 models in Table S1 are also used to compute model error, and the multimodel ensemble mean is also used to attribute changes in temperature due to one or a subset of forcings.

We consider the effects of GHG, natural influences (solar and volcanic), and other anthropogenic forcings (OA, mostly aerosols). Following the notation presented in equations (1)–(3), we have then  $X_{\text{GHG}}$ ,  $X_{\text{NAT}}$ , and  $X_{\text{OA}}$ , respectively, where the latter is calculated as  $X_{\text{OA}} = X_{\text{ALL}} - X_{\text{NAT}} - X_{\text{GHG}}$ . To calculate the covariance matrices  $\hat{\Sigma}_Y$ ,  $\hat{\Sigma}_{X_{\text{GHG}}}$ ,  $\hat{\Sigma}_{X_{\text{NAT}}}$ , and  $\hat{\Sigma}_{X_{\text{OA}}}$ , the covariance matrix for internal variability ( $\hat{\Sigma}_v$ ) is required. This is done by calculating the within-ensemble differences from the large CESM ensemble. In order to be consistent with the OLS approach,  $\hat{\Sigma}_v$  is split into two covariance matrices, one used to prewhiten the data and other for uncertainty estimates in  $\hat{\beta}_{\text{OLS}}$ . This is achieved by splitting the members from the large ensemble into two subsets of 17 members and then calculating  $\hat{\Sigma}_{v_1}$  and  $\hat{\Sigma}_{v_2}$  using this subset of simulations.

To determine which of the different errors is dominant, we carry our three main analyses: (1) using only internal variability to compute  $\hat{\Sigma}_Y$  and  $\hat{\Sigma}_{X_i}$ , (2) including observational error ( $\hat{\Sigma}_{\text{obs}}$ ) from CRUTEM4 for the estimation of  $\hat{\Sigma}_Y$ , and (3) including model errors ( $\hat{\Sigma}_m$ ) for the estimation of  $X_{\text{GHG}}$ ,  $X_{\text{NAT}}$ , and  $X_{\text{OA}}$ . The covariance matrices for internal variability ( $\hat{\Sigma}_{v_1}$  and  $\hat{\Sigma}_{v_2}$ ) are calculated using the regularization approach described in section 2.2 and as used in Ribes et al. (2013), as a means to obtain a better estimate of the sample covariance matrix. In order to calculate the observational uncertainty  $\hat{\Sigma}_{\text{obs}}$ , we consider the correlated error by using 100 ensemble members of the land-only component of HadCRUT4 and the uncorrelated errors from the same data set using the method described in Morice et al. (2012). The model error covariance matrix  $\hat{\Sigma}_m$  is conservatively estimated using the “models are statistically indistinguishable from the truth” paradigm as described in R17 Appendix—“Estimation of  $\Sigma_m$  and  $\Sigma_X$  with unbalanced data,” for each of the signals separately with the CMIP5 models that are indicated in Table S1. In all cases we assume that the mean values for  $X_i^*$  comes from the CESM-LE ensemble. This is done also on the third step, when the CMIP5 models are included to calculate  $\hat{\Sigma}_m$ , to make the analysis consistent with the previous steps. Therefore, for the third step we would have

$$\hat{\Sigma}_Y = \underbrace{\hat{\Sigma}_{\text{obs}}}_{\text{Observational error}} + \underbrace{\hat{\Sigma}_{v_1}}_{\text{Internal variability}} \quad (11)$$

$$\hat{\Sigma}_{X_i} = \underbrace{\left(1 + \frac{1}{n_m}\right) \hat{\Sigma}_m}_{\text{Model error}} + \underbrace{\frac{1}{n_m^2} \sum_{j=1}^{n_m} \frac{\hat{\Sigma}_{v_2}}{n_j}}_{\text{Internal variability}} \quad (12)$$

where  $n_m$  is the number of models and  $n_j$  is the number of ensembles for the  $j$ th model. We carry out a final analysis where we estimate  $X$  from the CMIP5 multimodel average. For the case in which we use CESM-LE as the model mean  $n_m = 1$  for calculating internal variability in equation (12) while when using CMIP5 multimodel mean  $n_m > 1$ , based on Table S1. Throughout this study, internal variability was computed from the CESM Large Ensemble.

From the best estimates calculated using the R17 methods, trends are estimated using linear regression. To compute the uncertainty range for these trends, 1,000 random samples are generated using the covariance matrices from equations (4) and (5) and the trends calculated from each sample. The 5% and 95% percentiles are considered as the lower and upper thresholds, respectively. For OLS, the model response is scaled by  $\hat{\beta}_{\text{OLS}}$  to calculate the trend by linear regression and estimate the warming/cooling rate to be compared with R17 best estimates ( $\hat{X}_i^*$  and  $\hat{Y}^*$ ) trends. We also show 5–95% ranges for OLS.

#### 4. Results and Discussion

The observed anomalies from CRUTEM4 (Figure 1b) show a warming trend, from the decadal averages, of 0.22 [0.15 to 0.31] °C per decade between 1955 and 2004 (1.1 [0.7 to 1.5] °C over 1955–2004). ALL captures

**Table 1**

*Hypothesis Testing  $\chi^2$  P Value for Individual Forcings From R17 Model in Cases Where (1) Internal Variability Only Was Used to Estimate the Covariance Matrices (iv only), (2) Inclusion of Observational Error (iv + obs), (3) Inclusion of Observational Error and Model Error (iv + obs + model), and (4) Considering the Multimodel Mean as the Ensemble Mean Instead of CESM Large Ensemble (MMM iv + obs + model)*

Forcing/error	iv only	iv + obs	iv + obs + model	MMM iv + obs + model
1955–2004				
Internal variability	0.00	0.00	0.00	0.00
OA	0.01	0.02	0.36	0.03
NAT	0.00	0.00	0.02	0.01
GHG	0.66	0.70	0.84	0.98
All forcings (GHG+NAT+OA)	0.70	0.73	0.96	0.96
ALL	0.35	0.43	0.74	0.86
1935–2004				
Internal variability	0.00	0.00	0.00	0.00
OA	0.00	0.00	0.00	0.00
NAT	0.00	0.00	0.01	0.00
GHG	0.73	0.78	0.92	0.95
All forcings (GHG+NAT+OA)	0.36	0.47	0.82	0.48
ALL	0.01	0.06	0.21	0.36

*Note.* The results presented here are for the 1955–2004 and 1935–2004 time window. GHG = greenhouse gas.

the observed warming with a correlation on annual time scales of 0.60 from 1955 to 2004 suggesting that about 40% of the observed interannual to multidecadal variability is forced. GHG has a similar trend when compared to CRUTEM4 and ALL simulation between 1955 and 2004, with a correlation of 0.39. This suggests that much of the observed temperature increase in Southeast Brazil could be due to GHG only. NAT and ALL suggests a slight cooling from the 1991 Pinatubo eruption in the early 1990s. The estimated OA signal cools until about 1980 and warms after that, with a linear correlation of 0.25 with observations in the 1955–2004 time window. This result might be due to changes in emissions of sulfur dioxide from Europe and North America that had rapidly increased starting in the beginning of the twentieth century and then declined from the 1970s due to emission control policies (Hoesly et al., 2018).

The best estimates  $\hat{Y}^*$  and  $\hat{X}_i^*$  are calculated using the R17 statistical model, using CESM as reference in three steps to understand the importance of the different types of uncertainties, as described in section 3: (1) using only internal variability (R17 iv only), (2) including observational error (R17 iv + obs), and (3) including model error (R17 iv + obs + model). After that, the linear trends in temperature using the raw model data and the R17 estimates for each of the three steps are estimated and compared.

Our results consistently find a detectable impact of GHG on Southeast Brazil temperature. Inclusion of observational error did not cause a significant increase in uncertainty suggesting that observational error is relatively unimportant. However, significant uncertainty comes from modeling uncertainty which affects the calculation of R17 best estimates. Approximately half of the uncertainty in the iv + obs + model case comes from model error. For example, uncertainties in CESM GHG forced trend for 1955–2004 are 2.1 times larger with all sources of error considered than with just internal variability.

The CESM OA response, with its small warming, and large uncertainties of  $-0.06$  to  $0.18$  °C due to model error, is consistent with the observed trends (Table 1). However, for the 1935 to 2004 time window OA makes no statistically significant contribution to the observed trends. Given this and the conservative estimates of model error for R17, we think that OA alone does not explain changes in Southeast Brazil.

Using CESM as the mean to define the forced signals and using all CMIP5 models to estimate  $\hat{\Sigma}_m$  may not be ideal because we assume a Gaussian uncertainty centered around CESM which lies toward the tail of the CMIP5 model distribution. Therefore, we use the R17 statistical model, considering all of the uncertainties, with the CMIP5 multimodel ensemble mean (R17 MMM iv + obs + model). Between 1955 and 2004 (Figure 2a), we also find a significant contribution to the observed warming from GHG. A trend of 0.19 to 0.30 °C per decade is found that is equivalent to a 0.95 to 1.50 °C warming in this 50-year period. NAT and

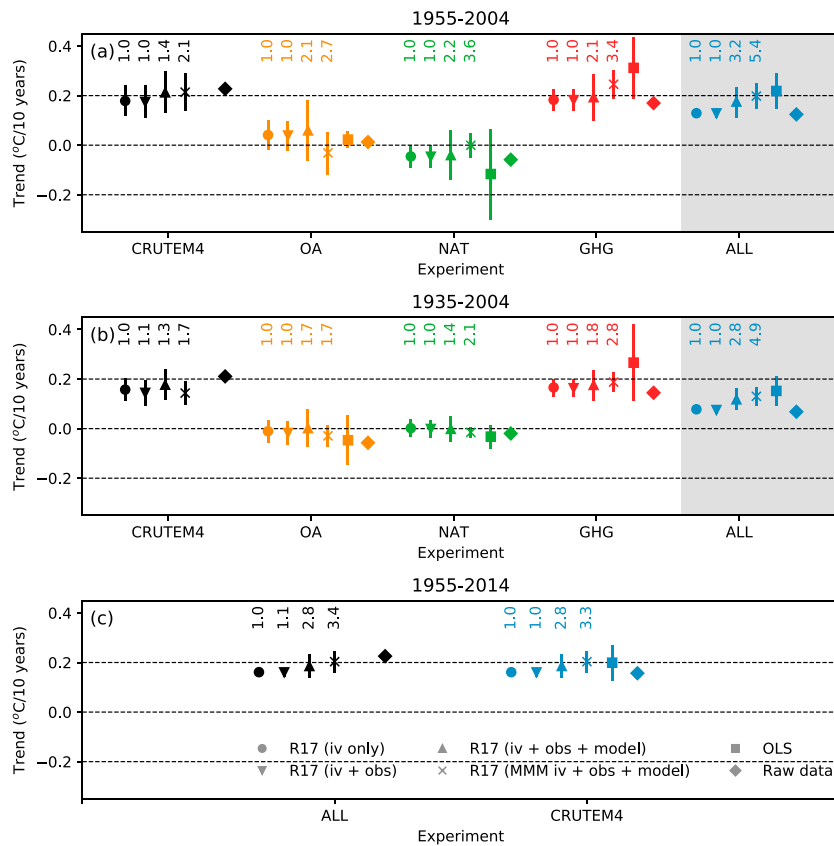


**Figure 2.** Temperature trends calculated from decadal averages for the observations (CRUTEM4) and each individual forcing (OA, NAT, and GHG) using R17 three signal models best estimates ( $\hat{X}_i^*$  and  $\hat{Y}^*$ ) for the different steps of analysis that include (1) internal variability only to estimate the covariance matrices (iv only, circle), (2) inclusion of observational error (iv + obs, triangle down), and (3) inclusion of observational error and model error (iv + obs + model, triangle up). The estimated trend using the multi model ensemble mean (MMM iv + obs + model, x symbol) and the CESM/CRUTEM4 raw data (diamond) are also included (raw data;  $X$  and  $Y$  from R17 notation) as well as the OLS estimate after scaling by  $\hat{\beta}_{OLS}$  (squares). The trends for ALL are based on R17 one signal model best estimates and are displayed in the shaded area in left of Figures 2a and 2b. (a) Trends between 1955 and 2004, (b) 1935 to 2004, and (c) 1955 to 2014 using RCP8.5 to extend the simulations after 2005. The numbers above the marker show the ratio between the uncertainty relative to the best estimate ( $X_i^*$  and  $Y^*$ ) of the iv-only case calculated as in equation (12).

OA are small and have significant uncertainties which makes it difficult to draw any conclusion regarding the impact of those forcings for this time scale and for the study region. Contrary to using CESM OA signal, CMIP5 OA multimodel ensemble mean does not show consistency with the observed warming in the 1955 to 2004 time window, with a trend of  $-0.07$  to  $0.01$  °C per decade.

Changing the time window of the analysis to begin in 1935 (Figure 2b) reduces the uncertainty bars, but results remain consistent with the 1955–2004 analysis. For the 1935–2004 time window the GHG trend is  $0.15$  to  $0.23$  °C per decade that is equal to a  $1.05$  to  $1.61$  °C warming in 70 years, which is also consistent with the observed trend. Our results are consistent with OLS (scaling factors in Figure S2) even though this estimate shows a higher positive trend and uncertainty for GHG. Using data from 1955 to 2014 from the ALL simulation increases the signal-to-noise ratio, reducing the uncertainty bars when considering model error, which implies that the simulated warming signal is more consistent across the different models. The results are also compatible with the observed trends which continues to imply a forced component.

## 5. Conclusions

The current study has used a novel Detection and Attribution method from Ribes et al. (2017) to attribute temperature changes of approximately  $1.1$  °C per 50 years for Southeast Brazil. Using the CMIP5 multimodel ensemble mean gave a trend of  $0.95$  to  $1.50$  °C per 50 years from GHG which suggests that anthropogenic

activities made a substantial contribution to the observed trend with no significant contribution from natural or non-GHG anthropogenic sources. The results seem to be robust to change in time window of the analysis and by taking account of both observational and model errors. Using CESM as the model mean to investigate which error is dominant in this analysis showed that more than half of the error may come from model uncertainty. It might be possible to reduce this uncertainty by rejecting some models that are very different from the observations. The inclusion of model error had a significant impact in the uncertainty of CESM OA warming signal for 1955–2004 which was not supported by the multimodel mean and by changes in the time window that did not reveal any contribution from other anthropogenic sources.

When other attribution studies are considered, we see that warming trend in Southeast Brazil due to anthropogenic activities is consistent with other regions. A trend of 0.19 to 0.30 °C per decade due to GHG was found in this study, with a small contribution from other anthropogenics, of –0.07 to 0.01 °C per decade. The IPCC AR5 reported an attributable warming trend of 0.08 to 0.21 °C, for global temperature, per decade due to GHG (Bindoff et al., 2013). GHG trends that are comparable to the overall anthropogenic trends for SE Brazil are consistent with regional studies for Western China, Canada, and Central England that showed attributable decadal warming trends due to anthropogenic activities of 0.19 to 0.30, 0.07 to 0.23, and 0.14 to 0.26 °C, respectively (Karoly & Stott, 2006; Wan et al., 2019; Wang et al., 2018). However, unlike these regional studies, we are able to calculate contributions from three different forcings. The results shown in this study, of a significant anthropogenic-induced warming in a regional scale, also suggest that human-induced climate change is becoming very strong at human relevant scales.

#### Acknowledgments

This study was carried out during Rafael C. de Abreu's scientific visit to the University of Edinburgh funded by the UK-Brazil Research & Innovation Partnership Fund through the Met Office Climate Science for Service Partnership (CSSP) Brazil as part of the Newton Fund. Simon F. B. Tett was supported by CSSP-Brazil. Rafael C. Abreu and Humberto R. Rocha acknowledges financing in part by FAPESP Project ClimateWise (2015/50682-6) and the Coordenação de Aperfeiçoamento de Pessoal de Nível Superior - Brasil (CAPES) – Finance Code 001, Project "Estimativa de evapotranspiração por sensoriamento remoto para gestão de recursos hídricos no Brasil" 88887.144979/2017-00. Andrew Schurer was supported by NERC under the Belmont forum, Grant PacMedy (NE/P006752/1). Part of the analysis was carried out using JASMIN data processing environment. We thank two reviewers for helpful comments, Aurélien Ribes for making code for the preprocessing of the data publicly available; Colin Morice for providing us with the land uncertainty data for HadCRUT4 and the World Climate Research Programme's Working Group on Coupled Modelling, which is responsible for CMIP; the climate modeling groups for producing and making available their model output; the U.S. Department of Energy's Program for Climate Model Diagnosis and Intercomparison; and the Global Organization for Earth System Science Portals for Earth System Science Portals. The code used in this study was made publicly available at the following address <https://github.com/rafaelcabreu/attribution> and includes the already processed time series used in this study.

#### References

- Allen, M. R., & Stott, P. (2003). Estimating signal amplitudes in optimal fingerprinting. Part I: Theory. *Climate Dynamics*, 21(5-6), 477–491.
- Allen, M. R., & Tett, S. F. (1999). Checking for model consistency in optimal fingerprinting. *Climate Dynamics*, 15(6), 419–434.
- Bindoff, N. L., Stott, P. A., AchutaRao, K. M., Allen, M. R., Gillett, N., Gutzler, D., et al. (2013). Detection and attribution of climate change: From global to regional. In T. F. Stocker, D. Qin, G.-K. Plattner, M. Tignor, S. K. Allen, J. Boschung, et al. (Eds.), *Climate change 2013: The physical science basis. Contribution of working group I to the fifth assessment report of the intergovernmental panel on climate change* (pp. 867–952). Cambridge, UK and New York: Cambridge University Press.
- Blain, G. C., Picoli, M. C. A., & Lulu, J. (2009). Análises estatísticas das tendências de elevação nas séries anuais de temperatura mínima do ar no Estado de São Paulo. *Bragantia*, 68(3), 807–815.
- Camargo, M. B. P. d. (2010). The impact of climatic variability and climate change on arabic coffee crop in Brazil. *Bragantia*, 69(1), 239–247.
- Coelho, C. A., de Oliveira, C. P., Ambrizzi, T., Reboita, M. S., Carpenedo, C. B., Campos, J. L. P. S., et al. (2016). The 2014 southeast Brazil austral summer drought: Regional scale mechanisms and teleconnections. *Climate Dynamics*, 46(11-12), 3737–3752.
- de Abreu, R. C., Cunningham, C., Rudorff, C. M., Rudorff, N., Abatan, A. A., Tett, S. F., et al. (2019). Contribution of anthropogenic climate change to April–May 2017 heavy precipitation over the Uruguay River basin. *Bulletin of the American Meteorological Society*, 100(1), S37–S41.
- Hegerl, G. C., von Storch, H., Hasselmann, K., Santer, B. D., Cubasch, U., & Jones, P. D. (1996). Detecting greenhouse-gas-induced climate change with an optimal fingerprint method. *Journal of Climate*, 9(10), 2281–2306.
- Hoelsy, R. M., Smith, S. J., Feng, L., Klimont, Z., Janssens-Maenhout, G., Pitkanen, T., et al. (2018). Historical (1750–2014) anthropogenic emissions of reactive gases and aerosols from the community emissions data system (CEDS). *Geoscientific Model Development (Online)*, 11, 369–408.
- Hurrell, J. W., Holland, M. M., Gent, P. R., Ghan, S., Kay, J. E., Kushner, P. J., et al. (2013). The Community Earth System Model: A framework for collaborative research. *Bulletin of the American Meteorological Society*, 94(9), 1339–1360.
- IBGE (2018a). Estimativas da População residente no Brasil e unidades da federação com data de referência em 1° de julho de 2018. Retrieved from <ftp://ftp.ibge.gov.br/EstimativasdePopulacao/Estimativas2018/estimativadou201820181019.pdf>
- IBGE (2018b). Produto Interno Bruto pela ótica da renda, Brasil, Grandes Regiões e as Unidades da Federação, pelas óticas da renda e da produção - 2010-2016. Retrieved from [ftp.ibge.gov.br/Contas\\_Regionais/2016/xls/PIB\\_Otica\\_da\\_Renda.xlsx](ftp.ibge.gov.br/Contas_Regionais/2016/xls/PIB_Otica_da_Renda.xlsx)
- Jones, P., Lister, D., Osborn, T., Harpham, C., Salmon, M., & Morice, C. (2012). Hemispheric and large-scale land-surface air temperature variations: An extensive revision and an update to 2010. *Journal of Geophysical Research*, 117, D05127. <https://doi.org/10.1029/2011JD017139>
- Karoly, D. J., & Stott, P. A. (2006). Anthropogenic warming of Central England temperature. *Atmospheric Science Letters*, 7(4), 81–85.
- Kay, J., Deser, C., Phillips, A., Mai, A., Hannay, C., Strand, G., et al. (2015). The Community Earth System Model (CESM) Large Ensemble project: A community resource for studying climate change in the presence of internal climate variability. *Bulletin of the American Meteorological Society*, 96(8), 1333–1349.
- Ledoit, O., & Wolf, M. (2004). A well-conditioned estimator for large-dimensional covariance matrices. *Journal of Multivariate Analysis*, 88(2), 365–411.
- Marengo, J. A. (2001). Mudanças climáticas globais e regionais: Avaliação do clima atual do Brasil e projeções de cenários climáticos do futuro. *Revista Brasileira de Meteorologia*, 16(1), 01–18.
- Morice, C. P., Kennedy, J. J., Rayner, N. A., & Jones, P. D. (2012). Quantifying uncertainties in global and regional temperature change using an ensemble of observational estimates: The HADCRUT4 data set. *Journal of Geophysical Research*, 117, D08101. <https://doi.org/10.1029/2011JD017187>
- Otto, F. E., Haustein, K., Uhe, P., Coelho, C. A., Aravequia, J. A., Almeida, W., et al. (2015). Factors other than climate change, main drivers of 2014/15 water shortage in southeast Brazil. *Bulletin of the American Meteorological Society*, 96(12), S35–S40.
- Ribes, A., Azañs, J.-M., & Planton, S. (2009). Adaptation of the optimal fingerprint method for climate change detection using a well-conditioned covariance matrix estimate. *Climate Dynamics*, 33(5), 707–722.



- Ribes, A., Planton, S., & Terray, L. (2013). Application of regularised optimal fingerprinting to attribution. Part I: Method, properties and idealised analysis. *Climate Dynamics*, *41*(11-12), 2817–2836.
- Ribes, A., Zwiers, F. W., Azais, J.-M., & Naveau, P. (2017). A new statistical approach to climate change detection and attribution. *Climate Dynamics*, *48*(1-2), 367–386.
- Silva Dias, M. A., Dias, J., Carvalho, L. M., Freitas, E. D., & Silva Dias, P. L. (2013). Changes in extreme daily rainfall for S ao Paulo, Brazil. *Climatic Change*, *116*(3-4), 705–722.
- Vincent, L. A., Peterson, T., Barros, V., Marino, M., Rusticucci, M., Carrasco, G, et al. (2005). Observed trends in indices of daily temperature extremes in South America 1960–2000. *Journal of Climate*, *18*(23), 5011–5023.
- Wan, H., Zhang, X., & Zwiers, F. (2019). Human influence on Canadian temperatures. *Climate Dynamics*, *52*(1-2), 479–494.
- Wang, Z., Jiang, Y., Wan, H., Yan, J., & Zhang, X. (2017). Detection and attribution of changes in extreme temperatures at regional scale. *Journal of Climate*, *30*(17), 7035–7047.
- Wang, Y., Sun, Y., Hu, T., Qin, D., & Song, L. (2018). Attribution of temperature changes in western China. *International Journal of Climatology*, *38*(2), 742–750.